ELSEVIER

Physica B 267–268 (1999) 277–284

PHYSICA B

Decoherence, dephasing and depolarization

H. Rauch[a,*], M. Suda[b], S. Pascazio[c]

[a]*Atominstitut der Österreichischen Universitäten, Schuettelstrasse 115, A-1020 Wien, Austria*
[b]*Österreichisches Forschungszentrum, A-2444 Seibersdorf, Austria*
[c]*Dipartimento di Fisica, Università di Bari, I-70126 Bari, Italy*

Abstract

By means of a quantum optical description the connection between decoherence, dephasing and depolarization is shown. The transition from a quantum state to a mixture is caused by the interaction of the neutron with fluctuating and dissipative forces in matter or magnetic fields. An analytical description of this effect provides the basis for phase sensitive investigations of condensed matter with polarized neutrons. Analogies between the coherence function and the beam polarization will be discussed. © 1999 Elsevier Science B.V. All rights reserved.

PACS: 03.75.D; 03.75.B; 42.50

Keywords: Decoherence; Neutron; Dephasing; Depolarization

1. Introduction

Neutron optics has been developed mainly on the basis of geometrical ray optics and has become an important tool for advanced beam tailoring including polarized beam techniques [1]. More recently, steps towards a quantum optics formulation of various phenomena opened a new field of research where dressed neutron states, non-classical and squeezed neutron states play an important role [2–4]. Neutron interference and neutron spin–echo experiments are the most typical examples in which phase-space considerations and quantum optical formulations shed new light on the neutron as a quantum entity rather than a classical particle or a classical dipole [5,6]. The related quantum phenomena can be described in analogy to the known formulations for light, atom and molecular optics [7–9]. Thus we can connect neutron optical phenomenon to a broader and rather topical field of research and we switch from a scattering theory based description to a quantum optical one.

Neutron depolarization became a standard technique for the investigation of magnetic domains and magnetic field distributions in condensed matter research [10–12]. Dephasing in neutron interferometer experiments is a rather similar effect effective to all kinds of inhomogeneities in a sample [13,14]. But depolarization and dephasing effects have a much broader impact on our understanding of physical effects, because they are relevant for the transition between the quantum and the classical

* Corresponding author.

PII: S0921-4526(99)00082-4

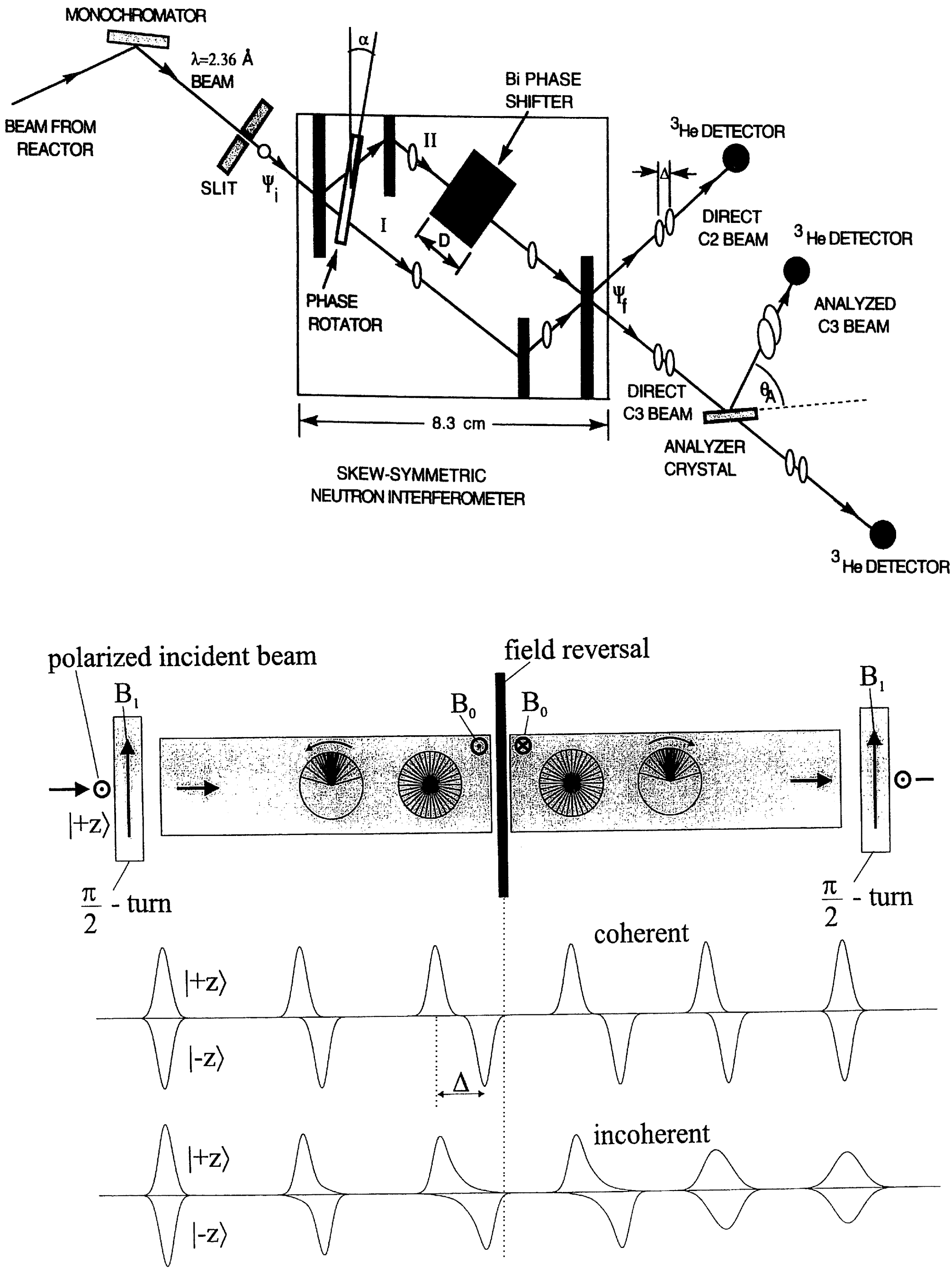

Fig. 1. Formation of Schrödinger cat-like states in interferometry (above) and in spin–echo arrangements (below) when spatial phase shifts are applied which are larger than the coherence lengths.

world which is equivalent to the transition between a quantum state and a classical mixture (e.g. [15–17]). In the following sections, we will notice that dephasing and depolarization effects become more dominant when highly non-classical states, e.g. Schrödinger cat-like states, are considered as they exist in interference and spin–echo systems [18]. In this case the wave packet becomes double peaked and the neutron occupies both spatially separated parts (see Fig. 1). It will be shown that vanishing contrast in an interferometer experiment and vanishing polarization in spin–echo systems do not necessarily mean dephasing or decoherence because proper post-selection methods can retrieve the coherence properties. Real dephasing requires an interaction of the quantum system with statistical fluctuations and/or dissipative systems.

2. Quantum optics formulation

Here we describe stationary situations which are described by the first-order two-point autocorrelation function relating the physical situations at $\boldsymbol{r}$ and $\boldsymbol{r}'$ [19,8]

$$G^{(1)}(\boldsymbol{r},\boldsymbol{r}') = \mathrm{Tr}\{\rho\Psi^{*}(\boldsymbol{r})\cdot\psi(\boldsymbol{r}')\}, \tag{1}$$

where ρ denotes the density matrix which describes the spatial profile of the beam and $\psi(\boldsymbol{r})$ is the solution of the time-independent Schrödinger equation which can be written in form of a wave packet

$$\psi(\boldsymbol{r}) \propto \int a(\boldsymbol{k})\mathrm{e}^{i\boldsymbol{k}\cdot\boldsymbol{r}}\mathrm{d}\boldsymbol{k}. \tag{2}$$

The amplitude function $a(\boldsymbol{k})$ determines the momentum distribution functions in the different directions $g(\boldsymbol{k}) = |a(\boldsymbol{k})|^2$. In an interference or spin–echo experiment one always has two beams (beam paths I and II or spin-up and spin-down states; Fig. 1) and, therefore, the intensity after superposition has to be calculated with the wave function

$$\psi(\boldsymbol{R}) = \psi^{I}(\boldsymbol{r}) + \psi^{II}(\boldsymbol{r}'). \tag{3}$$

This gives according to $I \propto |\psi(\boldsymbol{R})|^2$

$$I \propto G^{(1)}(\boldsymbol{r},\boldsymbol{r}) + G^{(1)}(\boldsymbol{r}',\boldsymbol{r}') + 2\,\mathrm{Re}\,G^{(1)}(\boldsymbol{r},\boldsymbol{r}'). \tag{4}$$

$G^{(1)}(\boldsymbol{r},\boldsymbol{r}) = I_1$ and $G^{(1)}(\boldsymbol{r}',\boldsymbol{r}') = I_2$ denote the intensities coming from both beams and $G^{(1)}(\boldsymbol{r},\boldsymbol{r}')$ defines the first-order correlation function, most commonly known as the coherence function

$$\Gamma^{(1)}(\boldsymbol{r},\boldsymbol{r}') = G^{(1)}(\boldsymbol{r},\boldsymbol{r}')/I = \Gamma(\boldsymbol{\Delta}) = (2\pi)^{-3/2}\int g(\boldsymbol{k})\mathrm{e}^{i\boldsymbol{k}\boldsymbol{r}}\,\mathrm{d}\boldsymbol{k}, \tag{5}$$

where a symmetric arrangement is considered $(I_1 = I_2 = I)$. $\boldsymbol{\Delta} = \boldsymbol{r} - \boldsymbol{r}'$ and $\Gamma(\boldsymbol{\Delta})$ can be written as $\Gamma(\boldsymbol{\Delta}) = |\Gamma(\boldsymbol{\Delta})|\exp(i\chi) = |\Gamma(\boldsymbol{\Delta})|\exp(i\boldsymbol{\Delta}\cdot\boldsymbol{k})$ and, therefore, one achieves

$$I \propto 1 + |\Gamma(\boldsymbol{\Delta})|\cos\chi(\boldsymbol{\Delta}). \tag{6}$$

$\chi = \boldsymbol{\Delta}\cdot\boldsymbol{k}$ denotes the phase shift where $\boldsymbol{\Delta}$ is the spatial phase shift between the two overlapping beams, both χ and $\boldsymbol{\Delta}$ can be calculated from the index of refraction. For nuclear and magnetic phase shifters these quantities read as

$$\Delta = \frac{2\pi N b_c D}{k^2} \quad \text{and} \quad \Delta_m = \frac{\mu m B D}{\hbar^2 k^2}, \tag{7}$$

where N and b_c denote the particle density and the coherent scattering length of the phase shifter, μ and m the magnetic moment and the mass of the neutron, B the strength of the magnetic field and D the thickness of the sample or the length of the magnetic field. The characteristical dimension of the absolute value of the coherence function $(|\Gamma(\boldsymbol{\Delta})|)$ determines the coherence length $\Delta^c = \Delta^c_x, \Delta^c_y, \Delta^c_z$, which obeys for Gaussian momentum distributions ($\triangleq$ coherent states) the Heisenberg uncertainty relation

$$\Delta^c_i \delta k_i = \tfrac{1}{2}. \tag{8}$$

For $\Delta_i \gg \Delta^c_i$ the coherence function goes to zero $|\Gamma(\Delta)| \to 0$, i.e. the interference contrast vanishes. Then, spatially separated packets appear (Schrödinger cat-like states) and the momentum distribution becomes modulated by a period $1/\Delta_i$, a phenomenon which has been verified experimentally as well [20,3,4]. For initially Gaussian packets having widths δx and δk, respectively, one obtains

$$I(x) = |\psi(x) + \psi(x+\Delta_0)|^2 = \exp[-x^2/2\delta x^2] + \exp[-(x+\Delta_0)^2/2\delta x^2]$$

$$+ 2\exp[-x^2/4\delta x^2] \times \exp[-(x+\Delta_0)^2/4\delta x^2]\cos(k\Delta_0) \quad (9a)$$

and

$$I(k) \propto \exp[-(k-k_0)^2/2\delta k^2][1+\cos(\mathbf{k}\cdot\mathbf{\Delta}_0)]. \quad (9b)$$

When one calculates the widths of the related distribution functions one notices that $\langle(\Delta k)^2\rangle$ can become smaller than the coherent state value $(\delta k)^2$ for $\Delta_0 = 0$. This means interferometric squeezing created by the superposition of two coherent states [21–23]. These highly non-classical states are made by the power of the quantum mechanical superposition principle.

A proper visualization of such states can be achieved by means of Wigner quasi-distribution functions which are defined as [24,25]

$$W_s(x,k,\Delta_0) = \frac{1}{2\pi}\int_{-\infty}^{+\infty} e^{ik\Delta'}\,\psi^*\left(x+\frac{\Delta'}{2}\right) \times \psi\left(x-\frac{\Delta'}{2}\right)d\Delta'. \quad (10)$$

This representation has the unique feature that integration over one variable gives the distribution function of the other

$$\int W_s(x,k,\Delta_0)\,dk = |\psi(x,\Delta_0)|^2 \quad \text{and}$$
$$\int W_s(x,k,\Delta_0)\,dx = |\psi(k,\Delta_0)|^2. \quad (11)$$

Related calculations have been done for the interferometer case [26,27] and for the spin–echo case [18,28], which is more closely connected to polarized neutron physics. Spin–echo systems are often described by the Bloch equation only

$$\frac{d\mathbf{P}}{dt} = \gamma(\mathbf{P}\times\mathbf{B}), \quad (12)$$

where the polarization $\mathbf{P}$ is given as $\mathbf{P} = \mathrm{Tr}\{\rho\langle\psi^*|\boldsymbol{\sigma}|\psi\rangle\}$. The similarity of the definitions of the correlation (coherence) function (Eq. (5)) and the polarization should be mentioned. γ is the gyromagnetic ratio of the neutron ($\gamma = 2\mu/\hbar$). This equation accounts for the Larmor rotation, but it ignores the coupling of the spin space to the momentum space, which exists in the form of Zeeman coupling. Thus the wave function has to be written as a coherent superposition of wave function parallel and antiparallel to the magnetic field indicating the spin space and momentum space coupling, i.e. the Zeeman coupling [29] (see Fig. 1)

$$\psi = \int a_+(k)e^{i(k+\Delta k)x}\,dk|z\rangle + \int a_-(k)\,e^{i(k-\Delta k)x}\,|-z\rangle dk, \quad (13)$$

where $\Delta k = \mu m B/\hbar^2 k$. For Gaussian incident wave packets centered around $k_0 + \Delta k$ (i.e. $a^+(k)$) and around $k_0 - \Delta k$ (i.e. $a_-(k)$) one yields after some calculation the Wigner function behind the experimental set-up,

$$W_s(x,k) = \frac{1}{4\pi}\exp[-(k-k_0)^2/2\delta k^2]\{A_1 + A_{-1} + 2A_0\cos[2k\Delta k|x_1 - x_2|/k_0]\}, \quad (14)$$

where

$$A_\varepsilon = \exp\left\{-2\delta k^2\left[x - |x_1 - x_2|\left(1+\varepsilon\frac{\Delta k}{k}\right)\right]^2\right\}. \quad (15)$$

Such Wigner functions are shown in Fig. 2 for very slow neutrons where $\Delta k/k_0 = 0.25$ can be achieved by feasible magnetic field strength. The related distributions of the wave packets in ordinary space and momentum space are obtained by integration of Eq. (14) according to Eq. (11). A modulated intensity distribution according to Eq. (9b) is anticipated which has been verified experimentally and which can be taken as a fingerprint of a Schrödinger cat-like state [4,30]. From such measurements the Wigner function can be reconstructed, which is equivalent to a state function reconstruction [31]. The appearance of separated Schrödinger cat-like states and their retrieval in the second part of the spin–echo system is visible. The situation in an existing spin–echo spectrometer is shown in Fig. 3. The wiggles (smile) of the Wigner function appearing between the Schrödinger

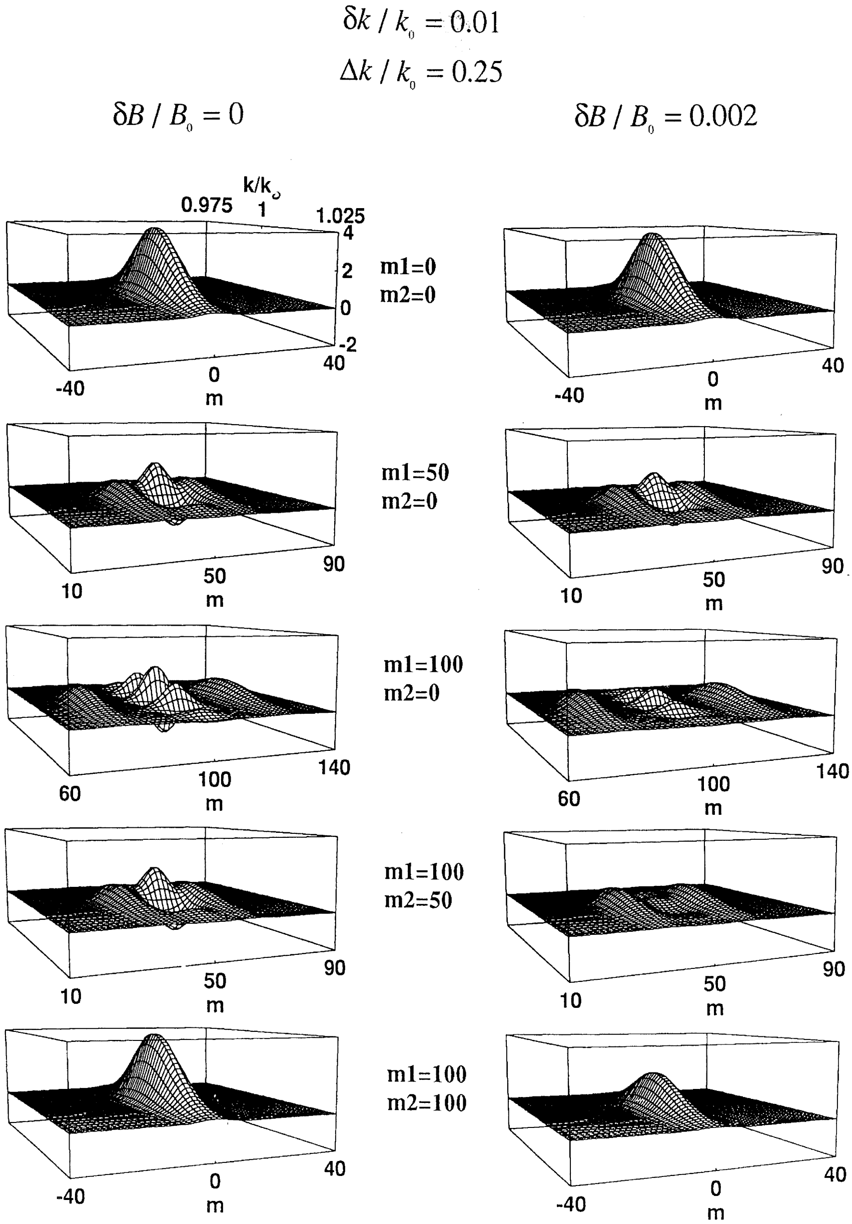

Fig. 2. Wigner functions within a spin–echo system without (left) and with (right) magnetic field fluctuations. m denotes the number of Larmor precessions ($m = \Delta kx$).

cat-like states indicate the non-classical features of these states. In existing spin–echo systems the spatial separation of the Schrödinger cat-like states reaches values up to 0.15 μm which is quite large compared to the widths of the incident packets ($\delta x \cong \Delta_c \cong 4$ nm). In the following section it will be shown how sensitive the wiggles of the Wigner-function are against any fluctuation and dissipative effects which account for depolarization and dephasing phenomena.

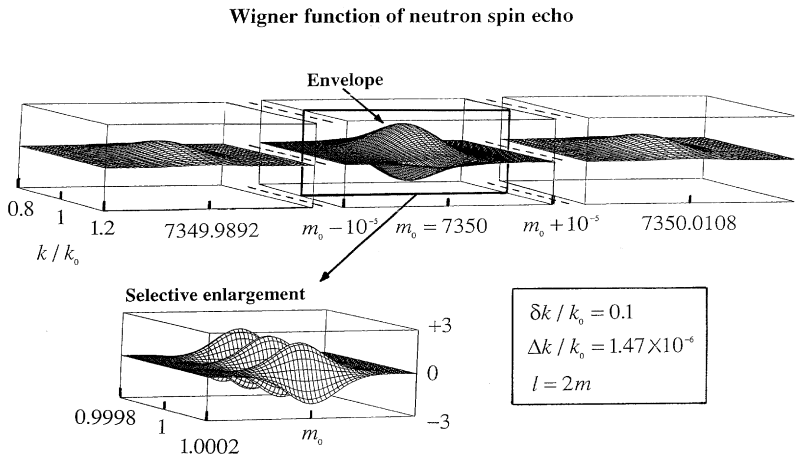

Fig. 3. Wigner function of an existing spin–echo spectrometer with a precession field integral of 0.5 Tm.

3. Dephasing effects

Dephasing effects occur due to the coupling of the quantum system to the environment ε depending on coordinates η which yield a wave function [15–17,32]

$$\psi = \psi_+ \times \varepsilon_+(\eta) + \psi_- \times \varepsilon_-(\eta). \tag{16}$$

When the environment acts on the phase only one obtains

$$\langle e^{i\chi} \rangle = \int P(\chi) e^{i\chi}\, d\chi = e^{i\langle\chi\rangle - \langle\delta\chi^2\rangle/2}, \tag{17}$$

where

$$\langle\chi\rangle = \int \chi\, P(\chi).\delta\chi \quad \text{and}$$

$$\langle\delta\chi^2\rangle = \int (\chi - \langle\chi\rangle)^2\, P(\chi)\, \delta\chi.$$

P being a probability distribution function taking into account dephasing effects due to environment. This causes additional damping $\exp[-\langle(\delta\chi)^2\rangle/2]$ to the interference term in Eqs. (4) and (6), to the momentum distribution in Eq. (9b) and to the Wigner function. Since the phase shift ($\chi = \boldsymbol{\Delta}\cdot\boldsymbol{k}$) is given by the path integral $\chi = (1/\hbar v)\oint V(\boldsymbol{r})\, d\boldsymbol{r}$, the average and the variances have to be taken by the related distribution function $P(\chi)$.

In spin–echo arrangements the magnetic field may have Gaussian variations around B_0 with a width δB. In this case the Wigner function has to be averaged over the distribution function $P(B)$ and one gets again Eq. (14) but with the following parameters:

$$A'_{1,-1} = A_{1,-1}^{(1+\beta^2)^{-1/2}} / \sqrt{1+\beta^2} \tag{18a}$$

$$A'_0 = A_0\, e^{-2(\delta B/B_0)^2 (k/k_0)^2 \Delta k^2 (x_1+x_2)^2}, \tag{18b}$$

with

$$\beta^2 = (\delta k/k_0)^2 (\delta B/B_0)^2 k_0^2 (x_1 + x_2)^2.$$

This causes a marked damping especially of the wiggles of the Wigner function as shown in Fig. 2. This is also equivalent to the transition from a quantum state to a mixture which is often called the depolarization effect.

When position-dependent field fluctuations are considered

$$P(B, B') = \frac{1}{2\pi(\delta B)^2 \sqrt{1-\rho^2}} \times \exp\{-[(B-B_0)^2 - 2\rho(B-B_0)(B'-B_0) + (B'-B_0)^2]/2(\delta B)^2(1-\rho^2)\} \tag{19}$$

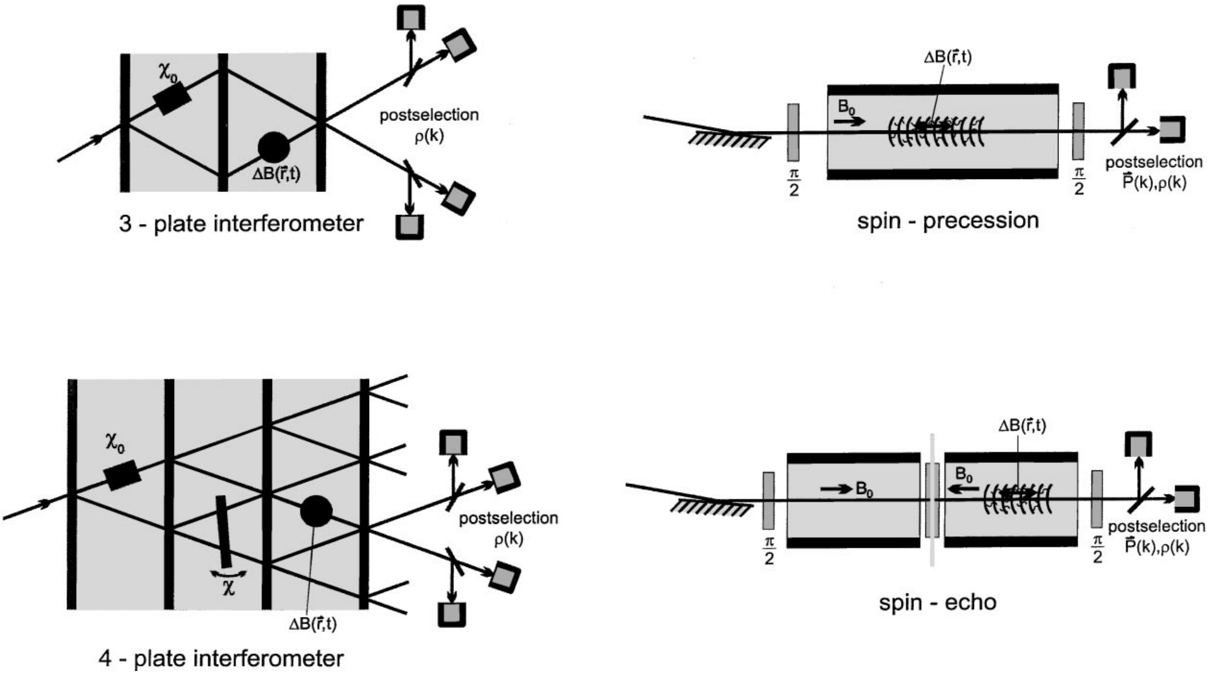

Fig. 4. Proposed dedicated dephasing experiments with interferometer and spin–echo systems.

$\rho \ldots$ correlation coefficient $(-1 \leqslant \rho \leqslant 1)$

the quantity β in Eqs. (18a) and (18b) has to be replaced by

$$\beta'^2 = \beta^2(1+\rho)/2, \tag{20}$$

which shows no damping for $\rho = -1$ (anticorrelated fluctuations) and maximum damping for $\rho = 1$.

4. Discussion

We have described decoherence, dephasing and depolarization in a quantum optics terminology where these phenomena are essential for the appearance of a classical world within quantum theory and for the understanding of the measurement problem. Formally this can be included in the quantum Liouville equation by a non-unitary term. For the density of states one achieves (e.g. Ref. [16])

$$i\frac{\partial \rho}{\partial t} = [H, \rho] - i\lambda[x, [x, p]], \tag{21}$$

which reads in the position representation

$$i\frac{\partial \rho(x, x', t)}{\partial t} = \frac{1}{2m}\left(\frac{\partial^2}{\partial x'^2} - \frac{\partial^2}{\partial x^2}\right)\rho - i\lambda(x - x')^2\rho \tag{22}$$

and which translates in the Wigner formalism into a diffusion equation in momentum space

$$\frac{\partial W_s(x, p, t)}{\partial t} = \Lambda\frac{\partial^2 W_s(x, p, t)}{\partial p^2}. \tag{23}$$

The Wigner functions can be measured by tomographic methods measuring the momentum distributions in interferometry and spin–echo systems as a function of the phase shifts. Related experiments applying modelled magnetic field fluctuations are in progress (Fig. 4). In all kind of such experiments one should keep in mind that the momentum distribution hitting the sample has a marked fine structure which varies strongly even by small variations of the phase shift, i.e. variations of the magnetic fields.

The quantum optics formalism shows how the entanglement of the spin, momentum and ordinary space exist in polarized neutron physics. The depolarization and dephasing effect has a much deeper impact on the understanding of the transition from the quantum to the classical world than it is usually thought when related measurements are used for condensed matter research.

Acknowledgements

This work has been supported by "Fonds zur Förderung der Wissenschaftlichen Forschung (Austrian Science Foundation)", project P10491, and the TMR-Network "Perfect Crystal Neutron Optics" (ERB-FMRX-CT96-0057).

References

[1] V.F. Sears, Neutron Optics, Oxford University Press, Oxford, 1989.
[2] E. Muskat, D. Dubbers, O. Schaerpf, Phys. Rev. Lett. 58 (1987) 2047.
[3] H. Rauch, Phys. Lett. A 173 (1993) 240.
[4] D.L. Jacobson, S.A. Werner, H. Rauch, A 49 (1994) 3196.
[5] F. Mezei, Physica B 151 (1988) 74.
[6] H. Rauch, J. Phys. Soc. Japan 65A (1996) 45.
[7] A. Born, E. Wolf, Principles of Optics, Pergamon Press, Oxford, 1975.
[8] D.F. Walls, G.J. Milburn, Quantum Optics, Springer, Berlin, 1994.
[9] L. Mandel, E. Wolf, Optical Coherence and Quantum Optics, Cambridge University Press, Cambridge, 1995.
[10] O. Halpern, T. Holstein, Phys. Rev. 59 (1941) 960.
[11] M.Th. Rekveldt, Z. Physik 259 (1973) 391.
[12] H. Leeb, M. Hochhold, G. Badurek, R.J. Buchelt, A. Schricker, Austral. J. Phys. 51 (1998) 401.
[13] G. Badurek, H. Rauch, A. Zeilinger, in: F. Mezei (Ed.), Neutron Spin Echo, Lect. Notes Phys., Vol. 128, Springer, Berlin, 1980, p. 136.
[14] H. Rauch, D. Tuppinger, Z. Physik A 322 (1985) 427.
[15] W.H. Zurek, Prog. Theoret. Phys. 89 (1993) 281.
[16] D. Giulini, E. Joos, C. Kiefer, J. Kupsch, I.-O. Stamatescu, H.D. Zeh, Decoherence and the Appearance of a Classical World in Quantum Theory, Springer, Berlin, 1996.
[17] M. Namiki, S. Pascazio, H. Nakazato, Decoherence and Quantum Measurement, World Scientific, Singapore, 1997.
[18] H. Rauch, M. Suda, Physica B 141–143 (1998) 157.
[19] R.J. Glauber, Phys. Rev. 130–131 (1963) 2766.
[20] H. Rauch, H. Wölwitsch, H. Kaiser, R. Clothier, S.A. Werner, Phys. Rev. A 53 (1996) 902.
[21] D.F. Walls, Nature 306 (1983) 141.
[22] W. Schleich, M. Pernigo, Fam Le Kien, Phys. Rev. A 44 (1991) 2172.
[23] G.S. Agarwal, D.F.V. James, J. Mod. Opt. 40 (1993) 1431.
[24] E.P. Wigner, Phys. Rev. 40 (1932) 749.
[25] H.W. Lee, Phys. Rep. 259 (1995) 147.
[26] M. Suda, Quantum Semiclass. Opt. 7 (1995) 901.
[27] H. Rauch, M. Suda, Appl. Phys. B 60 (1995) 181.
[28] M. Suda, H. Rauch, in: D. Han et al. (Eds.), Proceedings of the Fifth International Conference on Squeezed States and Uncertainty Relations, Balatonfüred, Hungary, NASA/CP-1998-206855.
[29] R. Gähler, R. Golub, K. Habicht, T. Keller, J. Felber, Physica B 229 (1996) 1.
[30] G. Badurek, H. Rauch, M. Suda, H. Weinfurter, in preparation.
[31] M. Freyberger, S.H. Kienle, V.P. Yakovlev, Phys. Rev. A 56 (1997) 195.
[32] A. Stern, Y. Aharonov, Y. Imry, Phys. Rev. A 41 (1990) 3436.